

Influence of In-Situ Scaling on Variability of Polluted Soil Erodibility Parameters

Al-Madhhachi, A. T.^{1*}, Hasan, M. B.²

1. Water Resources Engineering Department, Faculty of Engineering, Mustansiriyah University Baghdad 10047, Iraq
2. Environmental Engineering Department, Faculty of Engineering, Mustansiriyah University Baghdad 10047, Iraq

Received: 09.02.2018

Accepted: 21.03.2018

ABSTRACT: Middle and southern Iraq suffers from polluted soils due to crude oil, spilled on land, leakage from transmitting pipe networks, or petroleum products from refineries. Many researchers have studied pollution impacts on the soil in details, but there is a clear lack of investigation on the influence of crude oil on soil erodibility. Recent researches have investigated the influence of pollution on erodibility parameters, which include critical shear stress (τ_c) and detachment factor (d_c). The variability of d_c and τ_c due to different in-situ scaling has not been thoroughly established for polluted and unpolluted soils. Thus this research aims at investigating the influence of different in-situ scaling ratios (1:1, 1:30, and 1:50) on variability of d_c and τ_c for polluted and unpolluted soils under controlled laboratory conditions, using Jet Erosion Test (JET), and tries to compare the three solution techniques (namely, Blaisdell's approach, depth scour approach, and iterative approach) to solve d_c and τ_c from JETs for polluted and unpolluted soils. The polluted soil samples have been prepared by submerging the soil surface with crude oil for 24 hours prior to testing. Results show that there have been statistical differences in d_c and τ_c between polluted and unpolluted soil samples on the dry side of water contents with no statistically significant difference of measured d_c and τ_c being observed across different in-situ scale ratios for polluted and unpolluted soils. All told, the study shows less variability of measured d_c and τ_c across different solution techniques, compared to previous study findings.

Keywords: In-situ scaling, JET, Erodibility of polluted soils, Soil erodibility parameters, Crude oil.

INTRODUCTION

Landscape erodibility is gaining popularity, especially for polluted soils (Salah and Al-Madhhachi, 2016; Mutter et al., 2017; Shayannejad et al., 2017; Abbas et al., 2018). In streams, streambeds, and banks, contamination of natural water streams with sediment originates from erosion as

their central non-point source (Khanal et al., 2016). Soil contamination with crude oil, however, may occur from a natural or anthropogenic source. Naturally, oil seeps into the bottom of the ocean as a result of sediment rock erosion. Oil anthropogenic sources are usually from accidental oil spills due to human activities. This kind of oil leakage is generated from several sources, such as leakage from underground and aboveground storage tanks, transport

*Corresponding Author,
a.t.almadhhachi@uomustansiriyah.edu.iq

Email:

pipelines petroleum refineries, and power plants. Accidental rupture of huge transporting vessels, such as tanker trucks or ships, usually results in spillage of large quantities of oil into the environment. In Iraq, most crude oil spills have occurred due to terrorist explosions of crude oil transportation pipe networks. Oil leakage is an environmental problem that can adversely affect the landscape. Oil contact may change physical and chemical properties of the soil (Wang et al., 2013). Crude oil contamination increase hydrocarbon levels of the soil, raising its total organic carbon (Quyum et al., 2002). Wang et al. (2010) found that pollution with crude oil could increase the pH value of the soil. Spilled oil can inhibit plant growth, destroying micro-organisms of the soil (Labud et al., 2007; Sutton et al., 2013). Polluted soil from crude oil leakage may affect soil erodibility.

In the field of applied geomorphology, calculation of soil erosion rate has remained a challenging prospect for many engineers and scientists. Quantifying soil erosion is one of the most considerable difficulties for predicting deposit loads (Khanal et al., 2016). Generally, soil erodibility is approached via Excess Shear Stress (ESS) model, based on the hydraulic boundary shear stress (τ , Pa) along with two main empirical soil parameters, namely the detachment factor (d_c , $m^3/N s$) and critical shear stress (τ_c , Pa). Different laboratory-based experimental techniques have been utilized to determine soil erodibility parameters. Large and Small flumes (Hanson, 1990; Hanson & Cook, 2004; Briaud et al., 2001) have been employed to measure d_c and τ_c in-situ. Wan and Fell (2004) proposed laboratory hole erosion test to measure soil erodibility parameters. A Jet Erosion Test (JET) was proposed by Hanson and Hunt (2007) and Al-Madhhachi et al. (2013a, 2013b) to measure soil erosion parameters both in-situ and in laboratory. The laboratory hole

erosion test and JET are relatively newer techniques, while flumes are the traditional technique to estimate soil erosion parameters (Khanal et al., 2016).

Hanson (1990) developed the first version of a JET device (original JET), which was later advanced at USDA Hydraulic Lab in Stillwater, Oklahoma, to study erosion properties of a soil sample. Water jet is created by a persistent pressure, imposed on a soil surface in submerged circumstances. It applies a definite shear force on the soil surface, forming a scour hole (Khanal et al., 2016). The “mini” and original JET are the two recent versions of JETs. Hanson and Cook (1997, 2004) presented the description, testing methodology, and development of the mathematical approach for original JET. They also advanced an analytical procedure (1997) to attain a straight measure of τ_c and d_c , relying on diffusion principles via Excel spreadsheet. An inverse relation between τ_c and d_c of streambeds in the Midwestern U.S. was developed by Hanson and Simon (2001).

The “mini” JET is smaller in size and lighter in weight, requiring smaller amounts of water, in contrast with the original instrument. In comparison to “mini” JET, the handling and setting of the original instrument are harder in the laboratory and field environments. Simon et al. (2010) were the first to use “mini” JET device under field conditions. They reported differences in measured d_c and τ_c from the original and “mini” JET apparatus. Al-Madhhachi et al. (2013a) compared the “mini” and original JETs under laboratory settings, reporting some similarities among the devices in measured erosion parameters. Al-Madhhachi et al. (2013b) also confirmed employment of original and “mini” instruments in measuring soil detachment parameters with flume data tests.

The main benefits of the JETs are in-situ testing as well as their portability

throughout field sites. Daly et al. (2015b) analyzed watershed scale variability for JETs, performed at 13 sites of Illinois River basin in northeastern Oklahoma. The parameters of ESS model, also known as linear model, divide as much as three orders of magnitude across the watershed of the Illinois River. The changeability of the soil erosion parameters at the site scale were performed in another study by Daly et al. (2015a), who proposed that heterogeneity in different soil textures, macropores, soil moisture content, vegetation, in-situ scaling, and biochemical processes were the factors, contributing to the variability of soil detachment parameters. Khanal et al. (2016) quantified the inconsistency of erodibility parameters under organized laboratory settings in order to obtain a standard operation of “mini” JET device on remolded samples of two different soil textures. They found that the depth scour solution technique provided the least variability of erodibility parameters, compared to other techniques. Average value of d_c from laboratory tests of Khanal et al. (2016) was similar to those, predicted in the field by Daly et al. (2015a) that had similar soil textures. Therefore, the inconsistency can also be from complex collaborations of other components, such as the differences in scale between laboratory and field site testing. The variability of different in-situ scaling on estimating soil erodibility parameters has not been thoroughly established.

On the other hand, recent researchers have found that polluted soil is more erodible than clean or unpolluted soils (Salah and Al-Madhhachi, 2016; Mutter et al., 2017; Shayannejad et al., 2017; Abass et al., 2018). Increasing the erodibility of cohesive soils indicate that there is a defect, resulting from pollution in the environment (Mutter et al., 2017). The effect of lead contamination on soil detachment parameters by means of the

JET instrument has recently been investigated by Salah and Al-Madhhachi (2016), who saw that d_c rose as lead concentration was increased, whereas τ_c dropped. They found that contaminated soil is more unstable than unpolluted soils. Mutter et al. (2017) utilized 96 “mini” JETs to inspect the effect of three stabilizers on contaminated cohesive soil erodibility. Their results indicated that as the curing time increased, the d_c of the soil decreased for the same stabilizer percentage, while τ_c increased. Mutter et al. (2017) and Abbas et al. (2018) proved the benefit of using a “mini” JET device in consumption testing time and in testing soil stabilization due to soil contamination. Therefore, it is needed to investigate the variability of different in-situ scaling ratios on estimating soil erodibility parameters from both polluted and unpolluted soils under controlled laboratory conditions so that a benchmark can be established that enables the comparison of d_c and τ_c variability, observed in the field.

This research aims at investigating the variability of different in-situ scaling ratios (1:1, 1:30, and 1:50) on soil erodibility parameters (d_c and τ_c) at different water contents for polluted and unpolluted soils under controlled laboratory setups, using the “mini” JET device, as well as comparing the solution techniques, namely Blaisdell’s Approach (BA), Depth Scour Approach (DS), and Iterative Approach (IA), in deriving linear model parameters (d_c and τ_c) from JETs for polluted and unpolluted soils.

MATERIALS AND METHODS

ESS Equation was first introduced by Partheniades (1965). The ESS model is the most commonly employed sediment model in the literature (Khanal et al., 2016) and is expressed as:

$$\varepsilon_r = d_c (\tau - \tau_c)^a \quad (1)$$

where ε_r is the detachment rate in m/s; d_c ,

the detachment factor in $m^3/N.s$; τ_c , the critical shear stress in Pa; and a , an exponent equal to one, according to Hanson (1990).

Currently, detachment parameters of ESS formula are calculated, using three methods in analyzing JET data. Hanson and Cook (1997, 2004) developed Blaisdell's Approach (BA), regarded as the most popular technique. The fundamentals of fluid diffusion, the basic solution of BA, was advanced by Stein and Nett (1997). Blaisdell et al. (1981) developed a hyperbolic function to predict the depth progression of the scour hole. The analysis of the JET is focused on this suggestion that the ultimate stress value causes the greatest scour beneath the impinging jet. Hanson and Cook (2004) reported that the peak stress in the jet impingement zone was identical in amount to the design stress environment of the open channel. Therefore, the initial stress, τ_i , in the jet impingement zone is proposed as (Hanson and Cook, 1997, 2004):

$$\tau_i = \tau_o \left[\frac{S_p}{S_i} \right]^2 \quad (2a)$$

$$\tau_o = C_f \rho_w U_o^2 \quad (2b)$$

$$S_p = C_d d_o \quad (2c)$$

$$U_o = C \sqrt{2gh} \quad (2d)$$

where τ_i is the initial stress of jet impingement zone and τ_o , the supreme shear stress due to the jet velocity at the nozzle, both in Pa. Also, $C_f = 0.00416$ is the friction coefficient; ρ_w , the water density in kg/m^3 ; and U_o , the orifice jet velocity in m/s. Additionally, $C = 0.65$ is the discharge coefficient (Al-Madhhachi et al., 2013a), while g stands for acceleration due to gravity in m/s^2 and h represents the pressure head in m. As for S_p , it indicates the potential core length from jet origin in m, while $d_o = 3.18$ mm is the nozzle

diameter and $C_d = 6.3$ is the diffusion constant. The rate of variation in the depth of scour, dS/dt , was presumed as the erosion rate function for the highest stress at the boundary (Hanson and Cook, 1997). By replacing τ_i with τ and S_i with S (where S is the scour depth at each time, t), and inserting Equation 2a in Equation 1; the detachment rate formula for jet scour is expressed as (Hanson and Cook, 1997):

$$\frac{dS}{dt} = d_c \left[\frac{\tau_o S_p^2}{S^2} - \tau_c \right], \text{ for } S \geq S_p \quad (3)$$

when the rate of scour is equal to zero at the equilibrium depth, S_e , the critical shear stress can be expressed as (Hanson and Cook, 1997, 2004):

$$\tau_c = \tau_o \left(\frac{S_p}{S_e} \right)^2 \quad (4)$$

A long time is required to reach S_e ; therefore, it is challenging to define the scour depth equilibrium (S_e) (Blaisdell et al., 1981). Consequently, it has been determined depending upon scour depth data over time via the spreadsheet. The equilibrium scour depth can be assessed, utilizing a hyperbolic function, first advanced by Blaisdell et al. (1981), as follows:

$$X^2 = (f - f_o)^2 - A^2 \quad (5a)$$

$$X = \log \left(\frac{U_o t}{d_o} \right) \quad (5b)$$

$$f = \log \left(\frac{S}{d_o} \right) - \log \left(\frac{U_o t}{d_o} \right) \quad (5c)$$

$$S_e = d_o 10^{f_o} \quad (5d)$$

where A is the value for semi-transfer and semi-conjugation of the hyperbola. Microsoft Excel Solver can be used to predict A and f_o coefficients. This can be accomplished by fitting scour depth data, obtained from JETs' experiments, depending on plotting x against f . The

equilibrium depth, S_e , is known as the highest deepest scour hole, hence, beyond this hole the jet of water is not expected to cause any further erosion (estimated from Equation 5d). Equation 4 predetermines the τ_c parameter by establishing the S_e of scour hole from Blaisdell's function. By solving for the least squared deviation between the observed scour time (t) and anticipated time (T_p^*), the detachment factor d_c is then calculated via the following equation:

$$T^* - T_p^* = -S^* + 0.5 \ln \left(\frac{1+S^*}{1-S^*} \right) + S_p^* - 0.5 \ln \left(\frac{1+S_p^*}{1-S_p^*} \right) \quad (6)$$

where $T^* = t / T_r$ is the dimensional time and $T_r = S_e / (d_c \tau_c)$ is the reference time, as stated by Stein and Nett (1997), $S^* = S/S_e$; and $S_p^* = S_p/S_e$.

Alternatives to Blaisdell's Approach have recently been proposed in form of the Depth Scour Approach, DS, advanced by Daly et al. (2013), and Iterative Approach, IA, developed by Simon et al. (2010). The DS routine simultaneously searches for parameters d_c and τ_c to offer the best fit of observed JET data. Rewriting Equation 1 to examine the observed data in terms of scour depth against time of JET data will be as the following:

$$\varepsilon_r = \frac{dS_d}{dt} = d_c (\tau - \tau_c) \quad (7a)$$

Integrating Equation 7a overtime for estimating scour depth data could be expressed as:

$$S_d = d_c \int_{t_i}^t (\tau - \tau_c) dt \quad (7b)$$

where S_d is the depth of scour in cm at time t ; and t_i is the initial time in minutes. According to Hanson (1990), Equation 7b was designated for observed data to reduce the sensitivity of short-term oscillations. The mean of observed scour data against observed mean shear stress was presented in the integral form of Equation 7b;

therefore, this equation is reported as the series of readings (mean shear stress) against time for the N^{th} shear stress:

$$S_d = d_c \sum_{i=1}^N [(\tau - \tau_c) \Delta t]_i \quad (7b)$$

The parameters d_c and τ_c were estimated from observed scour data against time and shear stress. Equations 7 and 8 got incorporated in a spreadsheet tool, designated by Daly et al. (2013), in order to derive the ESS parameters (d_c and τ_c) from observed JET data. The IA solution was presented by Simon et al. (2010). It was configured by means of detachment parameters, calculated from Blaisdell's Approach. At the end of each experiment, the scour hole was expected to attain the S_e (Equation 5d). The τ_c was fixed at upper bound, utilizing this S_e . Then, the root mean square deviation was utilized to calculate τ_c and d_c in order to reduce the differences between observed and predict data (Khanal et al., 2016).

Remolded samples of soil sample, acquired from Al-Taji Region, northwest of Baghdad, got prepared for testing via "mini" JETs. Al-Madhhachi et al. (2013a) presented a detailed implementation and construction of "mini" JETs. The soil utilized for the remoulded samples was lean clay, the physical properties and chemical composition of which can be seen in Table (1). Distribution of the soil's particle size was analysed following ASTM Standard D422. Both liquid and plastic limits of the soils were determined, following ASTM standard D4318. Standard compaction tests were performed on the soils by means of ASTM standard D698A (ASTM, 2006). Table (1) also shows the physical and chemical compositions of the crude oil, used in this study. The crude oil was provided by Iraqi South Oil Company, Basrah. All chemical and physical properties of crude oil were tested and analysed at Iraqi South Oil Company laboratories. Other crude oil

properties were taken from the study by Ibrahim et al. (2010).

The soil specimen was first air dried and then sieved through a no. 4 sieve (4.75 mm). Afterwards, the soil specimen was blended with desired quantities of water to attain the selected soil moisture. In order to observe the variability of soil erodibility parameters at different soil moistures, three different soil moistures were selected in this study: dry side (W1), optimum side (W2), and wet side of optimum water content (W3) with 9.65%, 15.8%, and 20% moisture, respectively. The water quantities added to soil samples were 80g, 150g, and 190g of water per each 1000g of soils at W1, W2, and W3 of soil moisture contents, respectively. Also, soil quantities were 2000g, 59000g, and 98000g at 1:1, 1:30, and 1:50 scale ratios, respectively. While preparing for JET experiments, the samples were packed at three different in-situ scale ratios: 1:1, 1:30, and 1:50, to investigate the influence of in-situ scaling on the variability of soil erodibility parameters (Figure 1). For 1:1 scale ratio, the specimens were prepared by packing the soil into an ASTM standard mould (960 cm³ in volume) at three layers (25 blows

per layer) to achieve standard bulk density with three different soil moisture contents (W1, W2, and W3), as shown in Figure 1a. As for 1:30 scale ratio (Figure 1b), JET samples were arranged by packing the soil in a soil box, 49cm×49cm×12cm in size, at three layers of standard bulk density and with three different soil moisture contents (W1, W2, and W3). Finally, for 1:50 scale ratio (Figure 1c), the specimens were prepared by packing the soil into a soil box, 80cm ×50cm×12cm in size, at three layers of standard bulk density and with three different soil moisture contents (W1, W2, and W3).

The above procedure was performed for both polluted and unpolluted soils. The former received two to three centimeters of crude oil above the surface of the three scale ratios of its samples, following the packing procedure, and was left for 24 hrs. Afterwards, the extra crude oil was removed from the soil surface and soil samples were tested, using JETs. The reason behind removing the extra crude oil from the soil surface after 24 hrs, was to perform JET experiment without any disturbance.

Table 1. Physical properties and chemical composition of soils and the crude oil, used for the JETs

Source	USCS classification	Physical properties of soils						Standard Compaction		Specific gravity	pH
		Soil texture			Atterberg limits			Maximum Density, g/cm ³	Optimum water content (%)		
		Sand (%)	Silt (%)	Clay (%)	Liquid limit	Plastic limit	Plasticity index				
Al-Taji, northwest Baghdad	Lean Clay	15	55	30	38	26	14	1.88	15.80	2.50	7.5
Chemical compositions of soils, %											
Fe ₂ O ₃	P ₂ O ₅	SO ₃ ⁻²	Cl ⁻¹		CO ₃ ⁻²	OM		T.D.S	CaSO ₄	SO ₄ ⁻²	
4.09	0.74	0.28	0.11		0.20	1.09		0.66	0.60	0.34	
Physical and chemical compositions of crude oil											
Density, g/cm ³	Water cut, %	Specific gravity of water	Specific gravity of gas		Fluid temperature, C°		Pour Point*, C°		N ₂ , %	CO ₂ , %	
0.88	13	1.07	0.81		54		- 36		2.30	1.10	
American Petroleum Institute (API°)		Kinematic Viscosity* at 40°C, mm ² /sec	Conradson Carbon Content*, %		Sulfur Content*, %		Vanadium Content*, ppm		Nickel Content*, ppm	Ash*, %	
Density*											
33.60		6.90	4.10		1.95		23.90		16.41	0.01	

*Data were taken from Ibrahim et al. (2010).

For unpolluted soils, the soil samples were tested directly after the packing procedure, using the JET device. All thirty-six “mini” JETs were accomplished on the soil samples with a head setting of 90 cm. The running of JETs and collecting scour depth data versus recording time were performed, following Khanal et al. (2016) and Al-Madhhachi et al. (2013a) protocol. The JET data got analysed to derive erodibility parameters for linear model (ESS). The three solution techniques; BA, DS, and IA, were applied to derive erodibility parameters, utilizing the spreadsheet tool, established by Daly et al. (2013).

The computed statistical differences across the three different in-situ scale ratios (1:1, 1:30, and 1:50) were determined

through the analysis of variance (ANOVA) for the erodibility parameters at three different soil moisture contents (W1, W2, and W3). The mean, standard deviation, and the difference between the 25th and 75th percentiles (IQR) were described for τ_c and d_c . Pairwise comparison tests were carried out on the erodibility parameters, using Student-Newman-Keuls Method, revealed by ANOVA to have significant differences at a significance level of $\alpha = 0.05$. ANOVA was also employed to calculate the statistical significance differences across the three solution techniques (BA, DS, and IA) of three in-situ scale ratios (1:1, 1:30, and 1:50) at three soil moisture contents (W1, W2, and W3) of erosion parameters (τ_c and d_c).



Fig.1. Illustration of performing JET setup at different compacted soil scaling ratios: a) 1:1 scale, b) 1:30 scale, and c) 1:50 scale

RESULTS AND DISCUSSION

Similar to previous research findings (Al-Madhhachi et al., 2013a, 2013b; Al-Madhhachi, 2017), d_c dropped, as soil moisture content rose for all three solutions (BA, DS, and IA) along with all three in-situ scale ratios (Figures 2 to 4). The IQR of measured d_c at dry side of water content (W1) was greater than the one at optimum and wet sides of water contents (W2 and W3) for both polluted and unpolluted soils (Table 2). Moreover, the standard deviation and mean values of measured d_c at dry side of water content (W1) was greater than the one at optimum and wet sides of water contents (W2 and W3) for unpolluted soils, while there was no statistical difference in standard deviation and mean values of measured d_c across different water contents in all three solution techniques (BA, DS, and IA) for polluted soils (Table 2 and Figures 2 to 4).

Even though, it can be observed from Figures 2 and 3 that there were some differences between polluted and unpolluted soils in measured d_c at dry side of water content (W1), especially for 1:1 and 1:30 scale ratios, ANOVA reported that there were only statistical differences between polluted and unpolluted soils (with $P < 0.05$) at dry side (W1) of d_{c-BA} as well as

optimum side (W2) of d_{c-IA} (Table 2). Wang et al. (2013) reported that when coming into contact with soil, oil may change its physical-chemical properties. Also, Quyum et al. (2002) and Wang et al. (2010) found that crude oil contamination increased the hydrocarbon level of the soil and its pH. Therefore, this study proposed that chemical properties, blockage of the soil pores with crude oil, changes in soil pH, and high hydrocarbon levels in soils are the reasons for the differences in d_c between polluted and unpolluted soil samples.

Salah and Al-Madhhachi (2016) found that d_c increased as lead concentration rose. They proposed that lead particle oxidized to Pb^{+2} , getting adsorbed with soil particles. The cohesive forces declined between soil particles due to adsorption relation. In this study, the chemical properties, blockage of the soil pores with crude oil, changes in soil pH, and high hydrocarbon levels in soils reduced the detachment factor, especially at the dry side of water contents. Therefore, it is recommended to mix the components of crude oil with soils to increase the stability of packing roads, especially for dry soils. In general, there had not been any influence of soil water contents on erodibility parameters of polluted soils.

Table 2. Results of Normality Test (Shapiro-Wilk) across different in-situ scaling of soil samples (1:1, 1:30, and 1:50) of measured d_c for both polluted and unpolluted soil samples (n=6) at different water contents W1 (9.65%), W2 (15.8%), and W3 (20%) with different solution techniques

Detachment factor, $cm^3/N.s$	Water contents, %	Unpolluted soil				Polluted Soil				Polluted vs unpolluted soils
		Mean	Std Dev	IQR*	P-value	Mean	Std Dev	IQR*	P-value	P-value
d_{c-BA}	W1	4.14	1.02	1.86	0.83	1.47	0.88	1.41	0.44	<0.05
	W2	0.84	0.22	0.37	0.31	0.82	0.33	0.31	0.02	0.69
	W3	0.66	0.05	0.07	0.08	0.61	0.21	0.27	0.12	0.65
d_{c-DS}	W1	39.72	14.35	22.99	0.41	15.02	12.83	16.84	0.12	0.22
	W2	7.66	3.80	6.56	0.56	9.04	5.24	6.37	0.12	0.50
	W3	5.71	1.13	1.94	0.71	6.26	2.93	6.03	0.27	0.67
d_{c-IA}	W1	20.77	8.50	8.83	0.04	10.30	6.78	12.13	0.37	0.69
	W2	5.02	1.01	1.86	0.15	6.89	2.30	4.41	0.57	<0.05
	W3	5.06	1.34	2.24	0.57	6.44	3.18	4.78	0.52	0.24

Note: P-values > 0.05 indicate to there is not statistically significant difference.

*IQR = interquartile range, defined as the difference between the 25th and 75th percentiles.

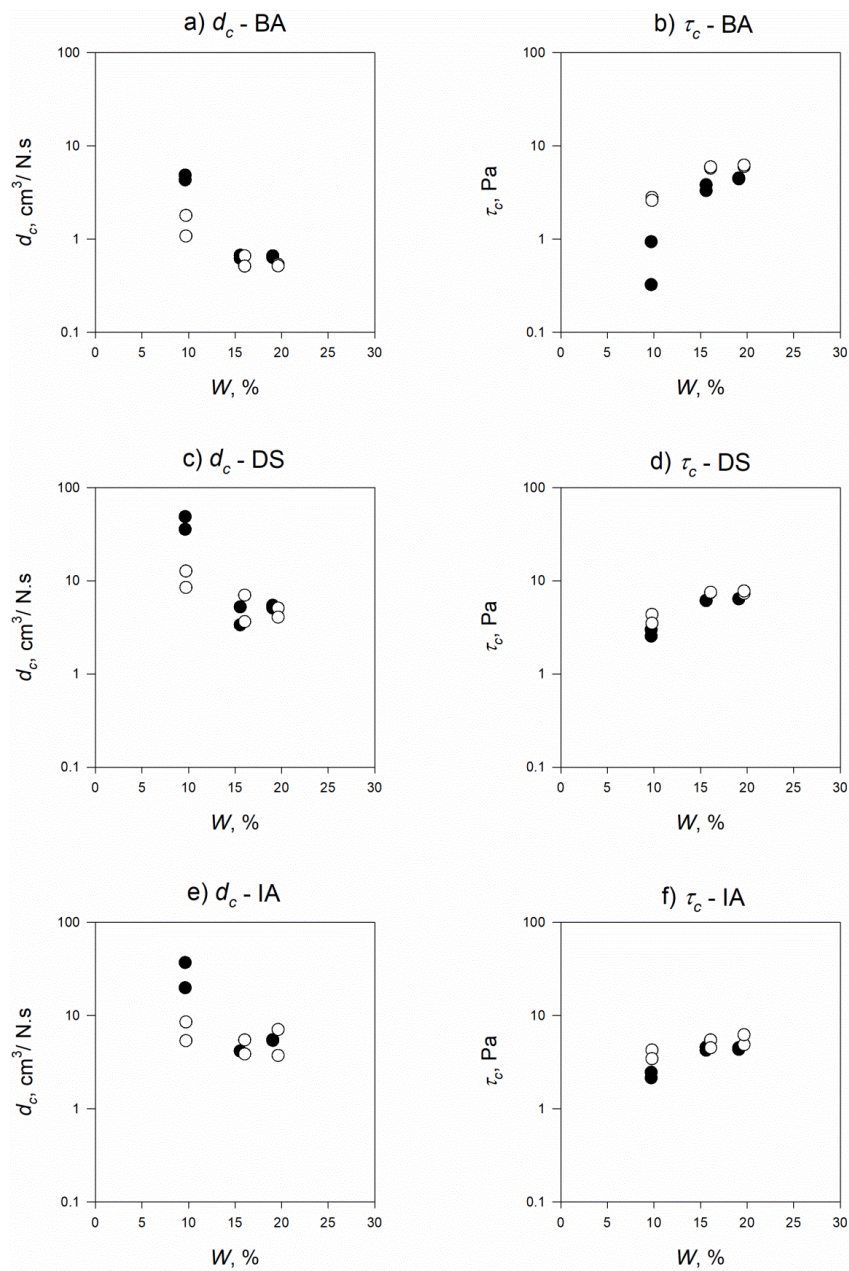


Fig. 2. Comparison of erodibility parameters between polluted and unpolluted soil samples from laboratory “mini” JETs for 1:1 scale ratio. BA = Blaisdell, DS = Depth Scour, and IA = Iterative approach. Note that solid-filled circles are for unpolluted soils and the empty ones for soils polluted by crude oil

Figures 2 to 4 demonstrate the comparison of τ_c between polluted and unpolluted soil samples at different in-situ scale ratios (1:1, 1:30, and 1:50) via different solution techniques (BA, DS, and IA), and with different soil moisture

contents (W1, W2, and W3). The τ_c rose as water content increased for unpolluted soils across all three approaches (BA, DS, and IA) at all three scale ratios, as observed in previous research findings (Al-Madhhachi et al., 2013a, 2013b; Al-Madhhachi, 2017).

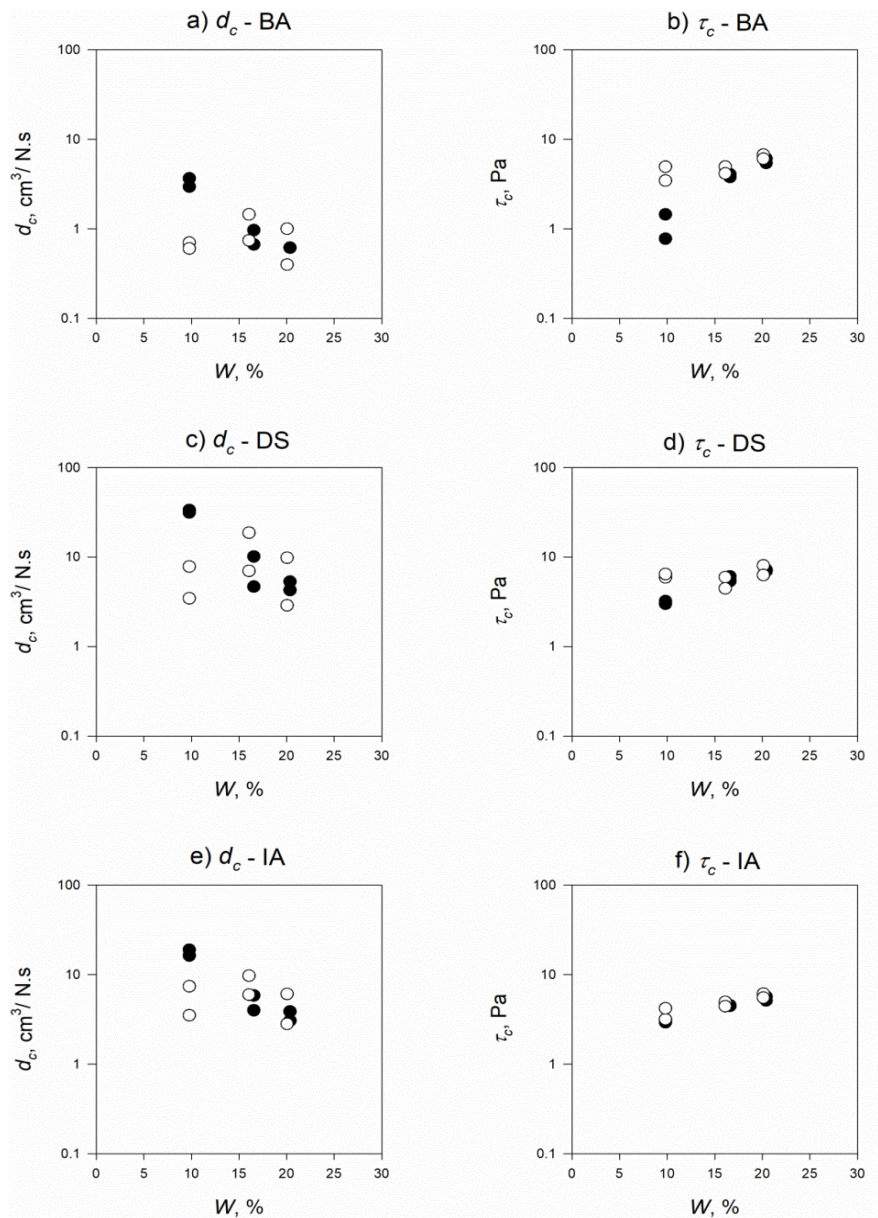


Fig. 3. Comparison of erodibility parameters between polluted and unpolluted soil samples from laboratory “mini” JETs for 1:30 scale ratio. BA = Blaisdell, DS = Depth Scour, and IA = Iterative approach. Note that solid-filled circles stand for unpolluted soils, while the empty one are for soils polluted by crude oil

As expected, the statistical description of τ_c indicated that the mean value of measured τ_{c-BA} at the dry side of water content (W1) was smaller than the one at optimum and wet sides of water contents (W2 and W3) for unpolluted soils (Table 3). ANOVA reported that there were statistically significant differences between polluted and unpolluted soils (with $P < 0.05$) at dry side (W1) of τ_c for all three

solution techniques as well as for wet side (W3) of τ_{c-BA} and τ_{c-IA} (Table 3). It can be observed from Figures 2a, 3a, and 4a that the measured τ_{c-BA} for all three scale ratios of unpolluted soil at W1 was below one for polluted soils. Again, chemical properties, blockage of the soil pores with crude oil, changes in soil pH, and high hydrocarbon levels are the reasons for the differences in τ_c between polluted and unpolluted soils.

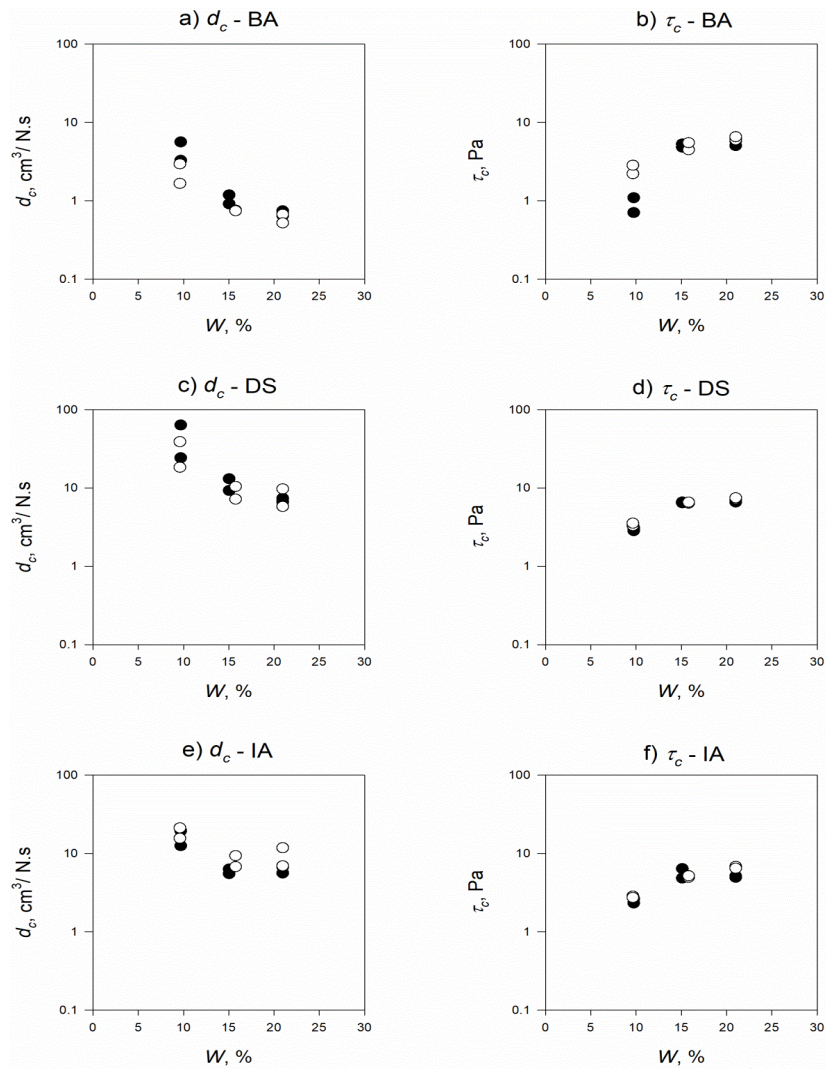


Fig. 4. Comparison of erodibility parameters between polluted and unpolluted soil samples from laboratory “mini” JETs for 1:50 scale ratio. BA = Blaisdell, DS = Depth Scour, and IA = Iterative approach. Note that solid-filled circles stand for unpolluted soils, while empty ones are for soils polluted by crude oil

Table 3. Results of Normality Test (Shapiro-Wilk) across different in-situ scaling of soil samples (1:1, 1:30, and 1:50) of measured τ_c for both polluted and unpolluted soil samples (n=6) at different water contents W1 (9.65%), W2 (15.8%), and W3 (20%) through different solution techniques

Critical shear stress, Pa	Water contents, %	Unpolluted soil				Polluted Soil				Polluted vs unpolluted soils
		Mean	Std Dev	IQR*	P-value	Mean	Std Dev	IQR*	P-value	P-value
τ_{c-BA}	W1	0.89	0.38	0.57	0.99	3.15	0.97	1.34	0.16	<0.05
	W2	4.21	0.74	1.29	0.58	5.16	0.73	1.42	0.60	0.12
	W3	5.25	0.68	1.38	0.64	6.29	0.32	0.61	0.13	<0.05
τ_{c-DS}	W1	2.95	0.23	0.35	0.64	4.53	1.36	2.62	0.12	<0.05
	W2	6.16	0.43	0.62	0.45	6.42	1.14	1.92	0.42	0.69
	W3	6.78	0.34	0.62	0.47	7.40	0.60	0.80	0.45	0.08
τ_{c-IA}	W1	2.61	0.37	0.70	0.88	3.46	0.66	1.39	0.28	<0.05
	W2	4.86	0.78	0.81	0.01	4.94	0.39	0.77	0.64	0.84
	W3	4.98	0.48	0.80	0.80	6.03	0.70	1.19	0.70	<0.05

Note: P-values > 0.05 indicate to there is not statistically significant difference.

*IQR = interquartile range, defined as the difference between the 25th and 75th percentiles.

Table 2 gives the influence of in-situ scaling ratios (1:1, 1:30, and 1:50) on measured d_c from different solution techniques (BA, DS, and IA) for both polluted and unpolluted soils. ANOVA showed that there was no statistical significance of measured d_{c-BA} , d_{c-DS} , and d_{c-IA} for unpolluted soils across different in-situ scale ratios, with the exception of d_{c-IA} with W1 (Table 2). Khanal et al. (2016) reported a much smaller variability of d_c than the one, described by Daly et al. (2015a) in their field studies on identical soil samples. Khanal et al. (2016) found that the variability in measured d_c for more cohesive soils was greater than the variability for less cohesive ones. Daly et al. (2015a) detected some inconsistencies in three orders of magnitude for measured d_c . Laboratory tests by Khanal et al. (2016) showed much less variability in measured d_c in comparison to the study by Daly et al. (2015a); however, Khanal et al. (2016) reported that the mean values of d_c resulted from the JET experiments on repacked and disturbed samples of the soil and the field JETs were noticeably analogous. Khanal et al. (2016) proposed factors like disturbance and repacking soil samples, soil texture heterogeneity, roots presence, soil moisture content, different head setting, and bulk density all involved in the variances, when predicting detachment parameters between the laboratory and in-situ experiments of JETs. In this study, under controlled laboratory setups, there had been no large-scale influence on the variability of d_c , compared with smaller scales. Similar to unpolluted soils, ANOVA showed that there was no statistical significance for polluted soils of measured d_{c-BA} , d_{c-DS} , and d_{c-IA} across all scale ratios, with the exception of d_{c-BA} with W2 (Table 2).

Table 3 gives the influence of in-situ scaling ratios (1:1, 1:30, and 1:50) on measured τ_c from different solution techniques (BA, DS, and IA) for polluted and unpolluted soils. ANOVA revealed

that parameters of polluted and unpolluted soils of τ_{c-BA} , τ_{c-DS} , and τ_{c-IA} were not significantly different across different scale ratios for all three water contents, except for τ_{c-IA} with W2 in unpolluted soils (Table 3). Again, Khanal et al. (2016) showed much less variability in measured τ_c , compared to the field studies by Daly et al. (2015a) on the same soil samples.

Disturbance and repacking soil samples, soil texture heterogeneity, roots presence, soil moisture content, different head setting, and bulk density are factors that contribute to the prediction of laboratory and field variances in erodibility parameters (Khanal et al., 2016). In general, there had been no large-scale influence on variability of measured τ_c , compared to smaller scales under controlled laboratory setups. No general arrangement was detected relative to the impact of diverse soil moisture contents on the τ_c of polluted soils across different scale ratios (Table 3). Measured τ_c of unpolluted soils at W1 was relatively lower than the one for other two water contents (W2 and W3).

The d_{c-BA} was an order of magnitude lesser than the equivalent d_c evaluated by DS and IA methods for both polluted and unpolluted soils and across different water contents (Figure 5), which was lower variability than those, observed in previous studies (Daly et al., 2015a; Khanal et al., 2016; Al-Madhhachi, 2017). Daly et al. (2015a) and Khanal et al. (2016) reported that d_{c-BA} was two orders of magnitude smaller than d_{c-DS} and d_{c-IA} on more cohesive soils. JETs variability under controlled laboratory conditions and under standard bulk density were much smaller than those, reported at uniform bulk density in the study by Khanal et al. (2016) as well as the field studies of Daly et al. (2015a) on more cohesive soils. Khanal et al. (2016) prepared two contrasting soils at uniform bulk densities of 1.7 Mg/m^3 (for less cohesive soil) and 1.4 Mg/m^3 (for more cohesive soil) at dry side of optimum

water contents to mimic the field condition of the same soils, used by Daly et al. (2015a). They performed 20 “mini” JETs on the two soil types, using different head settings. Daly et al. (2015a) noticed an inconsistency in around three orders of magnitude for d_c parameter, as reported in other researches (Wynn et al., 2008). In this study, pairwise comparison tests from ANOVA showed that d_{c-BA} , d_{c-DS} and d_{c-IA} parameters of unpolluted soils significantly differed across different in-situ scale ratios

and different water contents (W1, W2, and W3), with the exception of d_{c-DS} versus d_{c-IA} with W2 and W3 (Table 4). For polluted soils, pairwise comparison tests from ANOVA showed that d_{c-BA} versus d_{c-DS} and d_{c-BA} versus d_{c-IA} parameters were significantly different across different scale ratios and different water contents (W1, W2, and W3), while there was no statically-significant difference for d_{c-DS} versus d_{c-IA} of all water contents (Table 4).

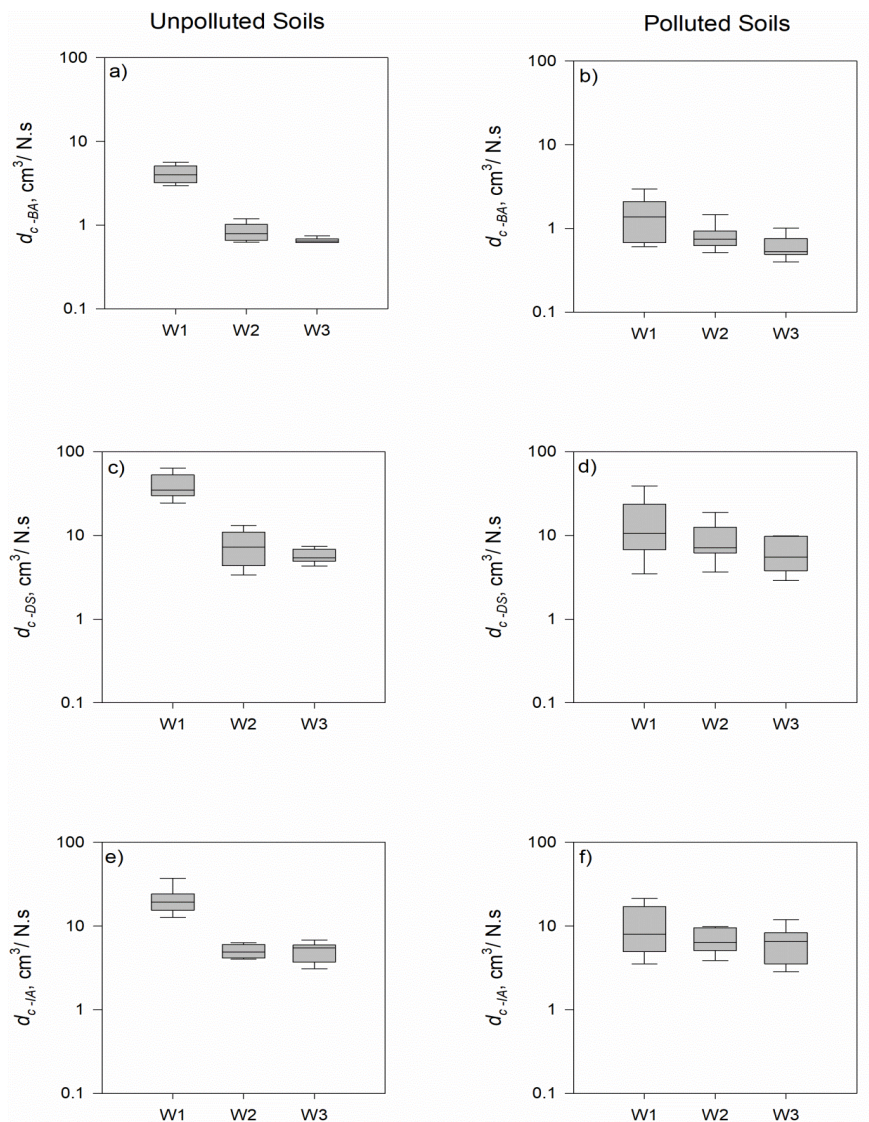


Fig. 5. Comparison of derived d_c from different solution approaches (BA, DS, and IA), using laboratory “mini” JETs of both polluted and unpolluted soil samples at different water contents, W1 (9.65%), W2 (15.8%), and W3 (20%), for three different scale ratios (1:1, 1:30, and 1:50). BA = Blaisdell, DS = Depth Scour, and IA = Iterative approach

Table 4. Results of Normality Test (Shapiro-Wilk) across different solution methods (BA, DS, and IA) of measured d_c for both polluted and unpolluted soil samples (n=18) with different water contents W1 (9.65%), W2 (15.8%), and W3 (20%) from different in-situ scaling. All pairwise multiple comparison results were performed, using Student-Newman-Keuls Method

Water contents, %	d_c , cm ³ /N.s	Unpolluted soil		Polluted Soil	
		Diff. of Mean	P-value	Diff. of Mean	P-value
W1	BA vs DS	35.585	<0.001	13.544	0.015
	DS vs IA	18.954	0.005	4.714	0.254
	BA vs IA	16.632	0.010	8.831	0.047
W2	BA vs DS	6.820	0.002	8.221	0.001
	DS vs IA	2.643	0.086	2.149	0.198
	BA vs IA	4.180	0.002	6.072	0.003
W3	BA vs DS	5.054	<0.001	5.825	0.001
	DS vs IA	0.654	0.167	0.173	0.879
	BA vs IA	4.400	<0.001	5.652	<0.001

Note: P-values > 0.05 indicate to there is not statistically significant difference.

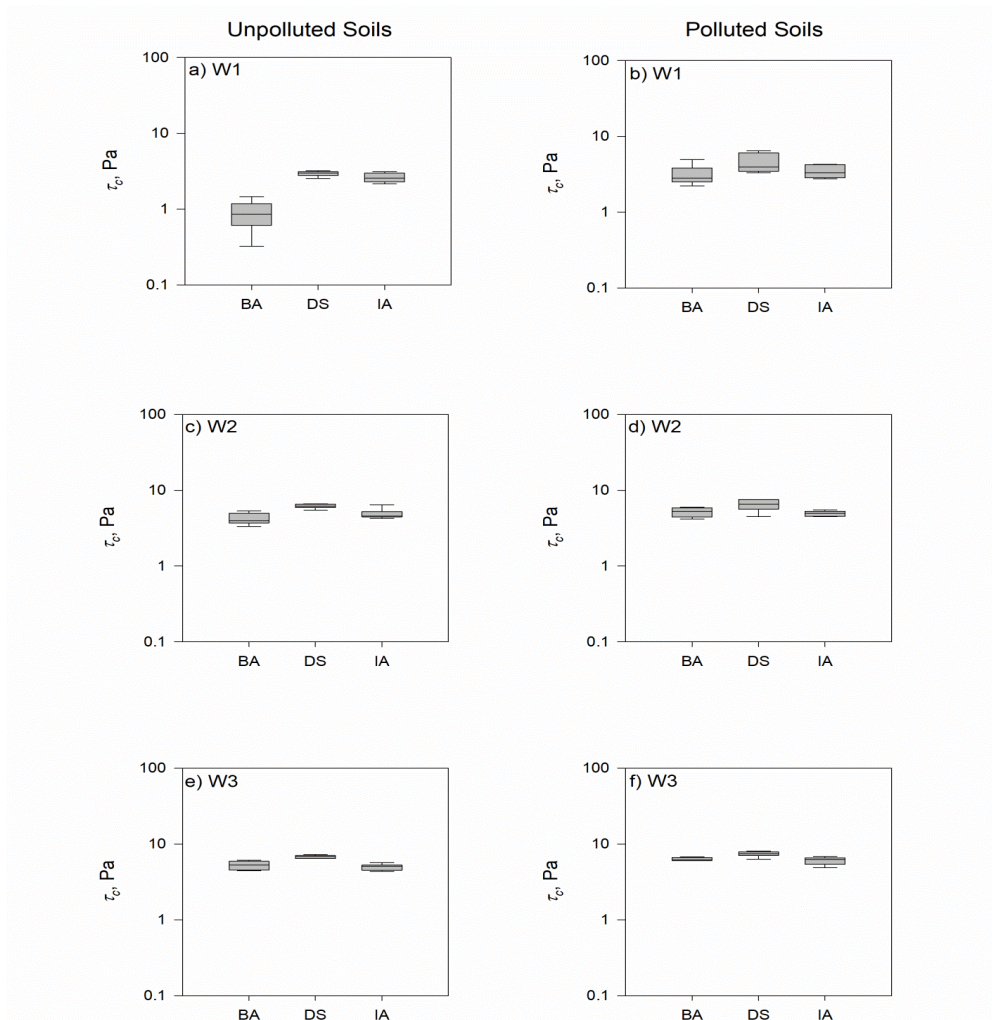


Fig. 6. Comparison of derived τ_c from different solution approaches (BA, DS, and IA), using laboratory “mini” JETs of both polluted and unpolluted soil samples at different water contents W1 (9.65%), W2 (15.8%), and W3 (20%) for three different scale ratios (1:1, 1:30, and 1:50). BA = Blaisdell, DS = Depth Scour, and IA = Iterative approach

There was no difference in the orders of magnitude across different solution techniques (BA, DS, and IA) of estimated τ_c for polluted and unpolluted soils, across different scale ratios and with different soil moisture contents (Figure 6), with the exception of τ_{c-BA} versus τ_{c-DS} and τ_{c-IA} at W1 (Figure 6a). This contradicted the previous findings of Daly et al., (2015a), Khanal et al. (2016), and Al-Madhhachi (2017), who proposed that τ_{c-DS} and τ_{c-IA} for the different soils were one order of magnitude greater than τ_{c-BA} . Khanal et al. (2016) reported that the differences in τ_c between the field tests and laboratory tests were larger for more cohesive soils, collected from Mile Creek

streambank than the one, proposed by Daly et al. (2015a). However, in this study, pairwise comparison tests from ANOVA revealed that the parameters of unpolluted soils (τ_{c-BA} , τ_{c-DS} , and τ_{c-IA}) differed significantly across different scale ratios and different water contents, except for τ_{c-BA} versus τ_{c-IA} of W3 (Table 5). For polluted soils, pairwise comparison tests from ANOVA showed that τ_{c-BA} versus τ_{c-DS} and τ_{c-DS} versus τ_{c-IA} parameters were significantly different across different scale ratios and different water contents, while there were no statistically-significant differences for τ_{c-BA} versus τ_{c-IA} of all water contents (Table 5).

Table 5. Results of Normality Test (Shapiro-Wilk), using One-Way Anova test by means of different solution methods (BA, DS, and IA) of measured τ_c for both polluted and unpolluted soil samples (n=18) with different water contents, W1 (9.65%), W2 (15.8%), and W3 (20%), from different in-situ scaling. All pairwise multiple comparison results were performed, using Student-Newman-Keuls Method

Water contents, %	τ_c , Pa	Unpolluted soil		Polluted Soil	
		Diff. of Mean	P-value	Diff. of Mean	P-value
W1	BA vs DS	2.066	<0.001	1.371	0.010
	DS vs IA	0.338	0.031	1.067	0.016
	BA vs IA	1.728	<0.001	0.303	0.427
W2	BA vs DS	1.956	<0.001	1.486	0.003
	DS vs IA	1.304	<0.001	1.266	0.003
	BA vs IA	0.652	0.021	0.220	0.507
W3	BA vs DS	1.801	<0.001	1.365	0.001
	DS vs IA	1.528	<0.001	1.102	0.002
	BA vs IA	0.273	0.065	0.263	0.335

Note: P-values > 0.05 indicate to there is not statistically significant difference.

CONCLUSION

A miniature instrument of JET (“mini” JET) was implemented on remolded soil samples of three different in-situ scale ratios (1:1, 1:30, and 1:50) and with three different water contents, under precise laboratory settings, to measure the effect of different in-situ scale ratios on variability of erodibility parameters (d_c and τ_c) for both polluted and unpolluted soils. The polluted soils were prepared by adding two to three centimeters of crude oil to the surface of the three scale ratios of soil samples, followed by a packing procedure, then to be left for 24 hrs. The soil samples were 960, 28800, and 48000 cm³ in volume for 1:1, 1:30, and 1:50 scale ratios, respectively.

Results showed there were no statistical differences in measured erodibility parameters between polluted and unpolluted soils, excluding the dry side of water content, especially for 1:1 and 1:30 scale ratios. Chemical properties, blockage of the soil pores with crude oil, changes in soil pH, and high hydrocarbon levels in soils were the reasons for such variations. It is recommended in this study to mix the component of crude oil with soils to increase the stability of packing roads, especially for dry soils. No influence of soil water contents on erodibility parameters of polluted soils was observed. What is more, there was no large-scale influence on variability of erodibility parameters,

compared with smaller scales for polluted and unpolluted soils. No general arrangement was noticed relative to the impact of different water contents on the τ_c of polluted soils across different scale ratios. The d_{c-BA} was one order of magnitude lower than the d_c equivalent, valued by the IA and DS solutions for both polluted and unpolluted soils, across different water contents, which had less variability than what was observed in previous studies. There were no statistically-significant difference for d_{c-DS} versus d_{c-IA} of polluted and unpolluted soils across all water contents, with the exception of the dry side of unpolluted soils. There were no statistical differences of measured τ_{c-BA} versus τ_{c-IA} across different water content for polluted and unpolluted soils, excluding the dry side of unpolluted soils. In general, this study demonstrated less variability of measured d_c and τ_c across different solution techniques, compared to previous study findings.

Acknowledgement

The authors acknowledge the faculty and staff of the Hydraulic Laboratory and Soil Laboratory of the Faculty of Engineering, Mustansiriyah University (www.uomustansiriyah.edu.iq), for their valuable help, in fixing and sustaining the apparatus, utilized in this research. The authors also acknowledge the faculty and staff of Iraqi South Oil Company laboratories for providing, testing, and analyzing the crude oil, used in this study.

REFERENCES

Abbas, M. N., Al-Madhhachi, A. T. and Esmael, S. A. (2018). Quantifying Soil Erodibility Parameters Due to Wastewater Chemicals. *International Journal of Hydrology Science and Technology* (under press).

Al-Madhhachi, A. T. (2017). Variability in soil erodibility parameters of Tigris Riverbanks using linear and non-linear models. *Al-Nahrain Journal for Engineering Sciences*, 20(4); 959-969.

Al-Madhhachi, A. T., Hanson, G., Fox, G., Tyagi, A. and Bulut, R. (2013a). Measuring soil erodibility

using a laboratory "mini" JET. *Trans. ASABE*, 56(3); 901-910.

Al-Madhhachi, A. T., Hanson, G., Fox, G., Tyagi, A. and Bulut, R. (2013b). Deriving parameters of a fundamental detachment model for cohesive soils from flume and jet erosion tests. *Trans. ASABE*, 56(2); 489-504.

ASTM Standards. (2006). Section 4: Construction. In *Annual Book of ASTM Standards*. (Philadelphia, Pa: ASTM).

Blaisdell, F. W., Clayton, L. A. and Hebaus, C. G. (1981). Ultimate dimension of local scour. *J. Hydraulics Division, ASCE*, 107(3); 327-337.

Briaud, J. L., Ting, C. K., Chen, H. C., Han, S. W. and Kwak, K. W. (2001). Erosion function apparatus for scour rate predictions. *J. Geotech. and Geoenviron. Eng. Division, ASCE*, 127(2); 105-113.

Daly, E., Fox, G., Al-Madhhachi, A. and Miller, R. (2013). A scour depth approach for deriving erodibility parameters from Jet Erosion Tests. *Trans. ASABE*, 56(6); 1343-1351.

Daly, E., Fox, G., Enlow, H. and Storm, D. (2015a). Site-scale variability of streambank fluvial erodibility parameters as measured with a jet erosion test. *Hydro. Processes*, 29(26); 5451-5464.

Daly, E. R., Fox, G. A., Al-Madhhachi, A. T. and Storm, D. E. (2015b). Variability of fluvial erodibility parameters for streambanks on a watershed scale. *Geomorphology*, 231(0); 281-291.

Hanson, G. J. (1990). Surface erodibility of earthen channels at high stresses. II: Developing an in situ testing device. *T. ASAE*, 33(1); 132-137.

Hanson, G. and Cook, K. (1997). Development of excess shear stress parameters for circular jet testing. (Paper #972227 presented at ASAE, St. Joseph, Mich).

Hanson, G. and Cook, K. (2004). Apparatus, test procedures, and analytical methods to measure soil erodibility in situ. *Appl. Eng. Agr.*, 20(4); 455-462.

Hanson, G. and Hunt, S. (2007). Lessons learned using laboratory JET method to measure soil erodibility of compacted soils. *Appl. Eng. Agr.*, 23(3); 305-312.

Hanson, G. J. and Simon, A. (2001). Erodibility of cohesive streambeds in the loess area of the midwestern USA. *Hydrological processes*, 15(1); 23-38.

Ibrahim, M. M., Mohammed, A. A. and Jar-Allah, A. T. (2010). Kinetics of Sulfur, Vanadium and

- Nickel Removal from Basra Crude Oil Hydro Treating. *Tikrit Journal for Engineering Science*, 17(3); 1-14.
- Khanal, A., Fox, G. A. and Al-Madhhachi, A. T. (2016). Variability of erodibility parameters from laboratory mini Jet Erosion Tests. *Journal of Hydrologic Engineering*, ASCE, 21(10). [https://doi.org/10.1061/\(ASCE\)HE.1943-5584.0001404](https://doi.org/10.1061/(ASCE)HE.1943-5584.0001404).
- Labud, V., Garcia, C. and Hernandez, T. (2007). Effect of hydrocarbon pollution on the microbial properties of a sandy and a clay soil. *Chemosphere*, 66(10); 1863-1871.
- Mutter, G. M., Al-Madhhachi, A. T. and Rashed, R. R. (2017). Influence of soil stabilizing materials on lead polluted soils using Jet Erosion Tests. *International Journal of Integrated Engineering*, 9(1); 28-38.
- Partheniades, E. (1965). Erosion and deposition of cohesive soils. *J. Hydraul. Div., ASCE*, 91(1); 105-139.
- Quyum, A., Achari, G. and Goodman, R. H. (2002). Effect of wetting and drying and dilution on moisture migration through oil contaminated hydrophobic soils. *Science of the Total Environment*, 296(1), 77-87.
- Salah, M. and Al-Madhhachi, A. T. (2016). Influence of Lead Pollution on Cohesive Soil Erodibility using Jet Erosion Tests. *Environment and Natural Resources Research*, 6(1); 88-98.
- Shayannejad, M., Ostad, A. A., Ramesh, A., Singh, V. P. and Eslamian, S. (2017). Wastewater and Magnetized Wastewater Effects on Soil Erosion in Furrow Irrigation. *International Journal of Research Studies in Agricultural Sciences*, 3(8); 1-14.
- Simon, A., Thomas, R. and Klimetz, L. (2010). Comparison and experiences with field techniques to measure critical shear stress and erodibility of cohesive deposits. (Paper presented at 2nd Joint Federal Interagency Conference, Las Vegas, NV).
- Stein, O. and Nett, D. (1997). Impinging jet calibration of excess shear sediment detachment parameters. *Trans. ASAE*, 40(6); 1573-1580.
- Sutton, N. B., Maphosa, F., Morillo, J. A., Al-Soud, W. A., Langenhoff, A. A., Grotenhuis, T., Rijnaarts, H. and Smidt, H. (2013). Impact of long-term diesel contamination on soil microbial community structure. *Applied and Environmental Microbiology*, 79(2); 619-630.
- Wan, C. F. and Fell, R. (2004). Laboratory tests on the rate of piping erosion of soils in embankment dams. *Geotechnical Testing Journal*, 27(3); 295-303.
- Wang, X., Feng, J. and Zhao, J. (2010). Effects of crude oil residuals on soil chemical properties in oil sites, Momoge Wetland, China. *Environmental Monitoring and Assessment*, 161(1); 271-280.
- Wang, Y., Feng, J., Lin, Q., Lyu, X., Wang, X. and Wang, G. (2013). Effects of crude oil contamination on soil physical and chemical properties in Momoge wetland of China. *Chinese Geographical Science*, 23(6); 708-715.
- Wynn, T., Henderson, M. and Vaughan, D. (2008). Changes in streambank erodibility and critical shear stress due to subaerial processes along a headwater stream, southwestern Virginia, USA. *Geomorphology*, 97(3); 260-273.

